Journal of Earth Science, *Vol. 30*, *No. 4*, *p. 679–688*, *August 2019* *ISSN 1674-487X*
Printed in China
https://doi.org/10.1007/s12583-019-0872-2

Genesis of the Binh Do Pb-Zn Deposit in Northern Vietnam: Evidence from H-O-S-Pb Isotope Geochemistry

Chaowen Huang[1], **Huan Li***[1], **Chun-Kit Lai**[2, 3]

1. *Key Laboratory of Metallogenic Prediction of Nonferrous Metals and Geological Environment Monitoring*, *Ministry of Education*, *School of Geosciences and Info-Physics*, *Central South University*, *Changsha* 410083, *China*
2. *Faculty of Science*, *Universiti Brunei Darussalam*, *Gadong BE*1410, *Brunei Darussalam*
3. *Centre of Excellence in Ore Deposits* (*CODES*), *University of Tasmania*, *Hobart*, *Tasmania* 7001, *Australia*

Chaowen Huang: https://orcid.org/0000-0002-8861-5418; Huan Li: https://orcid.org/0000-0001-5211-8324

ABSTRACT: The Binh Do Pb-Zn deposit in the Phu Luong region (Thai Nguyen Province, northern Vietnam) is located on the southern margin of the South China Block. The fault-controlled Pb-Zn orebodies are mainly hosted in Upper Paleozoic carbonate formations. In order to reveal the mineralization type and metallogenesis of this deposit, multi-isotopic (S, Pb, H and O) analyses on typical ore and gangue minerals were conducted. The average ore sulfide $\delta^{34}S_{\sum S}$ value is 4.3‰, suggestive of magmatic sulfur. The ore sulfide Pb isotope compositions are homogeneous, with the $^{206}Pb/^{204}Pb$, $^{207}Pb/^{204}Pb$ and $^{208}Pb/^{204}Pb$ values of 18.501 to 18.673, 15.707 to 15.798, and 38.911 to 39.428, respectively. Lead isotope model ages of the ore sulfides (240–220 Ma) are consistent with the timing of regional Triassic S-type granite emplacement (250–220 Ma), suggesting that the metals may have been granite-derived. The quartz $\delta D_{V\text{-}SMOW}$ (-82.4‰ to -70.5‰) and $\delta^{18}O_{H_2O}$ (-0.4‰ to +6.4‰) values suggest that the ore-forming fluids were composed of mixed magmatic and meteoric waters. Combined with the geological features of the Pb-Zn deposit in the region, we propose that the Pb-Zn deposits belong to magmatic-hydrothermal type, rather than MVT-type as previously suggested. The Triassic granites may have contributed the ore-forming material and heat that drove the hydrothermal system. The ore-forming fluids may have migrated into interlayer faults and fractures of the carbonate strata, diluted by subsurface meteoric water and deposited successively the vein-type and stratiform-type Pb-Zn ores.

KEY WORDS: Binh Do deposit, northern Vietnam, Pb-Zn belt, Triassic granitoids, isotope, geochemistry.

0 INTRODUCTION

The Northern Vietnam Pb-Zn belt, situated on the southern margin of the South China block, is a key Pb-Zn province in eastern Indochina (Li et al., 2018a; Tan et al., 2018; Anh et al., 2012; Lu et al., 2009; Yan et al., 2006). A number of Pb-Zn deposits, such as Binh Do (Vietnamese: Bình Đô), Bình Chai, Lửng Hoài, Po Pen, Phia Khao, Bô Luông, Dèo An, Than Tàu, La Poin, Na Son and Cho Dìen have been discovered (Pham-Ngoc et al., 2016; Chen et al., 2014, 2013; Can et al., 2011; Wang et al., 2011; Ishihara et al., 2010; Won-In and Charusiri, 2003), contributing to 80% of the total Pb-Zn reserves (~20 Mt) in Vietnam (Anh et al., 2012). Isotope geochemical studies on these deposits are generally lacking (e.g., Anh et al., 2012; Ishihara et al., 2010; Tran et al., 2008). For example, Pb-S isotope data were only reported from the Cho Dìen deposit (Wang et al., 2015), and no H-O isotope data were reported from the entire region. This hampers our understanding on the ore deposit type(s) and metallogenesis of this Pb-Zn belt, notably on the question whether these Pb-Zn deposits are MVT-type or magmatic- hydrothermal-type (Anh et al., 2012).

In this paper, we present new field geological and multi-isotope (S, Pb, H, O) data from the Binh Do deposit, discuss the ore-forming fluid and material source, and explore any metallogenic links between the regional large-scale Pb-Zn mineralization and Triassic (Indosinian) granitic magmatism.

1 GEOLOGICAL SETTING AND STRATIGRAPHY

1.1 Regional Geology

Northern Vietnam is situated in the southern margin of the South China Block, bordered with the Indochina Block to the southwest along the Ailaoshan-Song Ma suture zone (Fig. 1a; Lai et al., 2014a, b). Pre-Cenozoic lithostratigraphy in this region mainly comprises Cambrian–Lower Ordovician, Silurian–Permian, Lower–Middle Triassic, Upper Triassic and Upper Mesozoic sequences (Fig. 1b; Xia et al., 2016; Gonez et al., 2012). The Cambrian–Lower Ordovician sequences are dominated by terrigenous carbonate and shallow marine clastic

*Corresponding author: lihuan@csu.edu.cn

Manuscript received November 11, 2018.
Manuscript accepted March 15, 2019.

sedimentary rocks mainly exposed in the western and southern parts of northern Vietnam (Lepvrier et al., 2011). The Silurian–Permian sequences are characterized by marine-facies sedimentation. There was likely a brief tectonic uplift episode in the Early–Late Permian, followed by a rapid marine transgression (Cheng et al., 2016; Findlay, 1997). The Lower–Middle Triassic sequences is mainly exposed in the Song Hien zone, dominated by turbidite deposits such as conglomerate, sandstone, shale and chert. In the Late Triassic, the region was uplifted due to the Triassic Indosinian orogeny, and the sedimentary rocks are composed mainly of molasse formation (Metcalfe, 2002). By the Late Mesozoic, graben deposition of terrigenous red sandstone occurred (Cai and Zhang, 2009).

Northern Vietnam had experienced multi-phase magmatic activities during the Ordovician–Silurian, Permian, Triassic and Cretaceous (Chen et al., 2014; Wang et al., 2011; Liu et al., 2007; Yan et al., 2006, 2003; Gilley et al., 2003; Carter et al., 2001; Roger et al., 2000). The Ordovician–Silurian magmatic rocks are mainly composed of the Song Chay granite complex and the Phan Ngame granite complex. The Song Chay complex is the largest granite complex (outcrop area: 2 500 km^2) in Vietnam, consisting mainly of diorite and medium-fine-grained foliated granite (zircon U-Pb ages: 465 to 424 Ma; Carter et al., 2001; Roger et al., 2000). The Permian magmatic rocks are mainly composed of ultramafic rocks, gabbro and granites, which have been interpreted as products of the Emeishan large igneous province (LIP) (Tran et al., 2008; Hanski et al., 2004; Polyakov et al., 1999). Triassic intrusions are widely distributed in the region, and zircon U-Pb dating on the post-collisional granites and granodiorite yielded ca. 252 to 245 Ma (Halpin et al., 2016; Chen et al., 2014). Cretaceous granitoids (ca. 94 to 87 Ma) are mainly distributed in the Tinh Tuc area north of the Bac Kan fault (Roger et al., 2012; Wang et al., 2011).

1.2 Ore Deposit Geology

The Binh Do Pb-Zn deposit is located in the NE-trending Ha Giang-Bac Kan fault zone, which lies in the southeastern part of the northern Vietnam Pb-Zn belt (Fig. 1b). Exposed stratigraphy at the mine includes the Cambrian sequence, Lower Devonian Song Cau Group, and the Mia Le and Khao Loc formations (Fig. 2a). Cambrian rocks are distributed in the southern part of the mine, and consist mainly of sandstone, siltstone, shale and mica schist with limestone interbeds. The Song Cau Group is distributed in the eastern part of the mine, and consists mainly of conglomerate, sandstone, siltstone, shale and limestone. The Mia Le Formation is distributed in the central and western parts of the mine and consists mainly of (argillaceous)-sandstone and (marly)-shale. The Khao Loc Formation (main ore host strata) is mainly composed of marble, chert and limestone. No magmatic rocks are reported at Binh Do.

The Pb-Zn orebodies at Binh Do are mostly hosted in carbonate sequences and controlled by faults. The orebodies can be divided into stratiform-type (No. I and No. II) and vein-type (No. III and No. IV), among which the stratiform

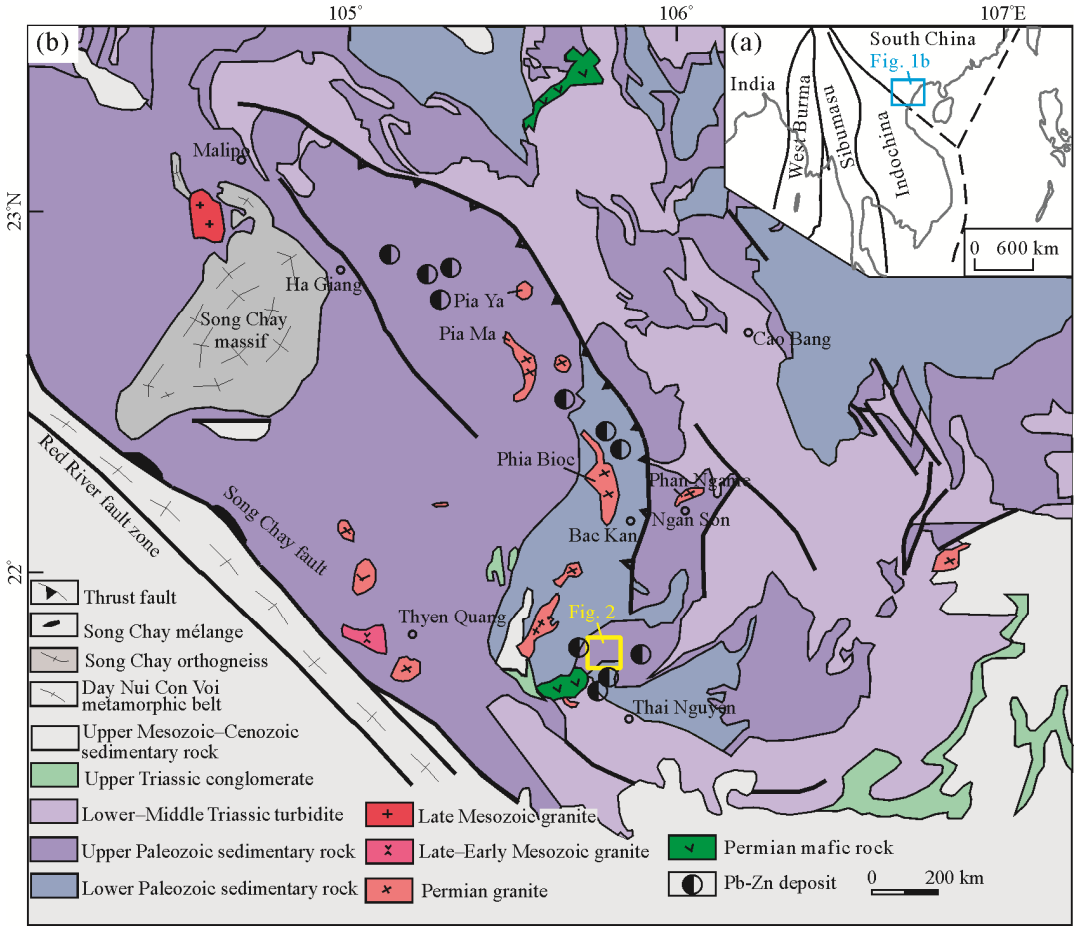

Figure 1. Regional geological map of the northern Vietnam Pb-Zn belt (modified after Chen et al., 2014).

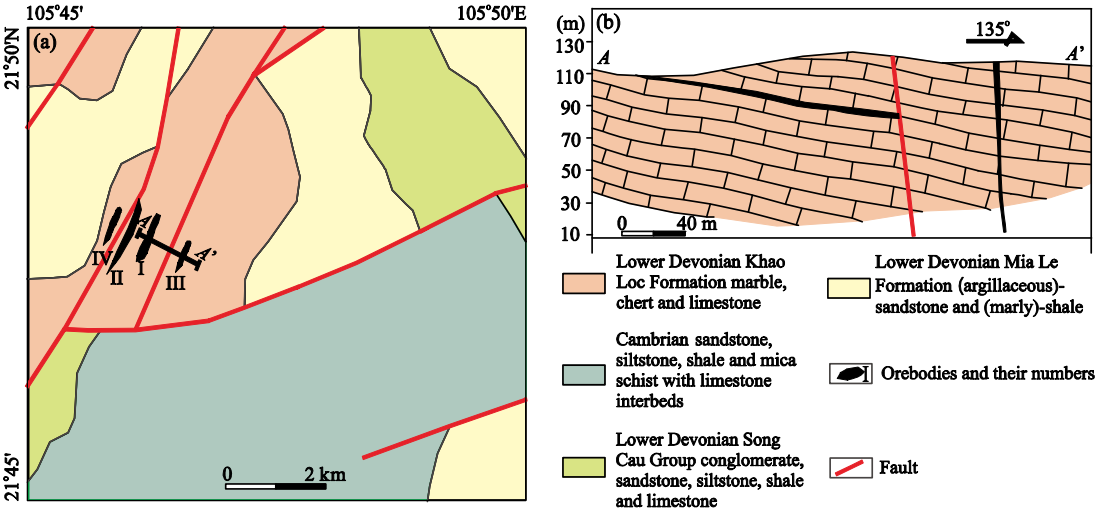

Figure 2. Simplified geological map (a) and cross section (b) of the Binh Do Pb-Zn deposit.

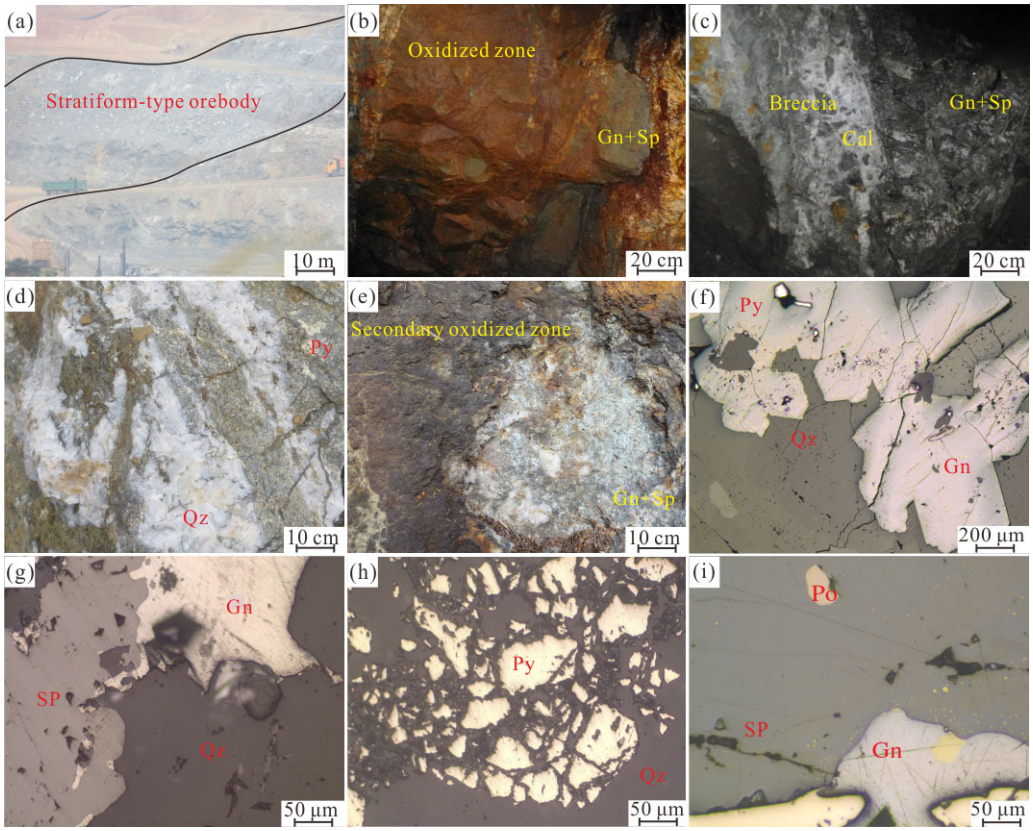

Figure 3. Field occurrences and photomicrographs of typical ores in the Binh Do Pb-Zn deposit. (a) Stratiform-type orebodies; (b) vein-type orebodies; (c) brecciated Pb-Zn ores; (d) disseminated Pb-Zn ores with strong pyritization; (e) secondary oxidization zones; (f) euhedral-subhedral galena intergrows with quartz; (g) euhedral galena and sphalerite intergrows with quartz; (h) disseminated pyrite in quartz; (i) xenomorphic sphalerite intergrows with galena and pyrrhotite. Gn. Galena; Sp. sphalerite; Py. pyrite; Po. pyrrhotite; Cal. calcite; Qz. quartz.

No. II orebody is the largest (Fig. 2a). The stratiform-type orebodies occur along stratigraphic interfaces (Fig. 2b), with a length of 0.8–1 km and a width of 20–50 m. The Pb-Zn ores from the stratiform-type orebodies are mainly banded (Fig. 3a) and massive. The vein-type orebodies develop along NNE-trending faults/fractures (Fig. 2b), having an outcropping length of 0.3–0.5 km and a width of 10–30 m. The ores are veined (Fig. 3b), brecciated (Fig. 3c) or disseminated (Fig. 3d). In addition, the stratiform-type orebodies and the vein-type orebodies are developed separately and no contact relations can be found (Fig. 2b). Thus, there is no way to determine whether they formed simultaneously or successively in the field. Moreover, supergene ores are also developed on/near the ground surface (Fig. 3e). Metallic minerals of the stratiform-type and vein-type orebodies are similar, and include mainly galena (Fig. 3f), sphalerite (Fig. 3g), pyrite (Fig. 3h) and rare pyrrhotite (Fig.

3i). These sulfide minerals intergrow with each other and possess hypidiomorphic and xenomorphic granular textures. Non-metallic minerals include mainly quartz and calcite. Boundaries between orebodies and wall rocks are clear and featured by an alteration halo. Major wall-rock alteration styles include silicification, carbonation and pyritization. Based on the paragenetic sequence of minerals, two stages of mineralization (hydrothermal stage and supergene stage) have been determined (Fig. 4).

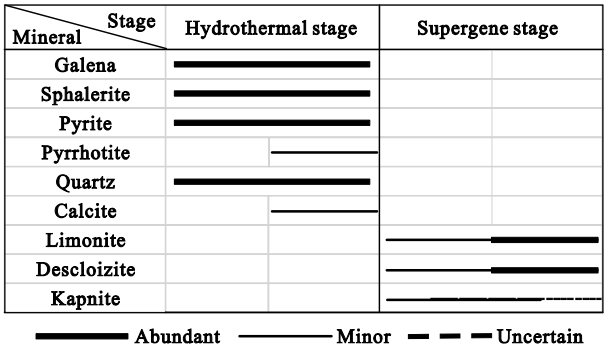

Figure 4. Paragenetic mineral sequences and ore-forming stages of the Binh Do Pb-Zn deposit.

2 ANALYTICAL METHODS

Samples were collected from underground tunnels in the Binh Do mining area, and we conducted S-Pb isotope analyses on sulfides and H-O isotope analyses on quartz. After the samples were crushed, washed and dried, minerals such as pyrite, galena, sphalerite and quartz were selected under the double eyepiece, with over 98% purity.

Hydrogen-oxygen isotope analyses were conducted at the Analytical Laboratory of BRIUG, using a Finningan MAT-253 mass spectrometer. Oxygen was extracted from quartz using a quantitative reaction with BrF_5 in externally heated nickel vessels at ca. 700 ºC and converted to CO_2 on a platinum-coated carbon rod. Analyses of the hydrogen isotopic compositions of fluid inclusions were conducted on the same quartz samples measured for oxygen isotopes. Quartz separates were first degassed of labile volatiles and secondary fluid inclusions by heating under vacuum to 120 ºC for 3 h. The released water was trapped and converted to hydrogen by passing over heated zinc, and then analyzed with the mass spectrometer. The detailed analytical procedures for H-O isotope analyses were described in Ni et al. (2017) and Li et al. (2013). The isotopic data are reported in per mil relative to the V-SMOW standards for oxygen and hydrogen, with an analytical precision of ±0.2‰ for $\delta^{18}O$, and ±2‰ for δD.

Sulfur and lead isotope analyses were conducted at the same laboratory. Sulfur isotope analyses were conducted using a MAT-251 EM mass spectrometer, with analytical procedures similar to Li et al. (2016). Pure sulfide samples (200-mesh) were combusted under vacuum with CuO in a 1 000 ºC oven. Liberated SO_2 was frozen in a liquid nitrogen trap after cryogenic separation from other gases. All values are reported as per mil (‰) relative to Canyon Diablo Troilite (CDT), with analysis accuracy better than ±0.2‰. The lead isotopic compositions of the sulfide samples were also analyzed on a MAT-261, using the method similarly described in Li et al. (2018b) and Xu et al. (2017). Sulfide samples were dissolved completely in ultrapure acids of HNO_3+HCl at 180 °C. The Pb in the samples was separated and purified using a two-column AG 1-X8 anion resin method. Pb isotopic ratios were corrected to reference values of Pb standard NBS-981 (Todt et al., 1996), with analytical reproducibility of ~0.1% (2σ) for $^{206}Pb/^{204}Pb$, $^{207}Pb/^{204}Pb$, and ~0.2 % (2σ) for $^{208}Pb/^{204}Pb$.

3 RESULTS

The analytical results of the S-Pb isotopes for 12 sulfide samples (4 pyrite, 4 galena and 4 sphalerite) are shown in Table 1. Taken together, there are no big differences in these values between the stratiform-type and vein-type ores. However, small variations can be still observed. Overall, the pyrite yielded the highest $\delta^{34}S$ values (+4.9‰ to +6.2‰), followed by galena ($\delta^{34}S$= +1.3‰ to +3.9‰) and sphalerite ($\delta^{34}S$= +2.3‰ to +3.6‰) (Fig. 5a). In addition, a weak decreasing trend in $\delta^{34}S$ values for galena and pyrite from stratiform-type ore to vein-type ore can be observed. Lead isotopes for all the sulfides are overall similar, with $^{206}Pb/^{204}Pb$=18.501–18.673, $^{207}Pb/^{204}Pb$= 15.707–15.798, and $^{208}Pb/^{204}Pb$=38.911–39.428. However, there is a slight decreasing trend in the $^{206}Pb/^{204}Pb$, $^{207}Pb/^{204}Pb$ and $^{208}Pb/^{204}Pb$ ratios for galena (and an increasing trend for sphalerite) from the stratiform-type to vein-type ore. The μ and ω values of all the sulfides range 9.66 to 9.83 and 38.97 to 41.00, respectively, with the Pb model ages ranging ca. 220 to 238 Ma (Table 1).

The H-O isotopic results of 6 quartz samples are shown in Table 2. The $\delta D_{V\text{-}SMOW}$ values range -82.4‰ to -70.5‰, and the $\delta^{18}O_{V\text{-}SMOW}$ values range +9.6‰ to +16.4‰ (corresponding $\delta^{18}O_{H2O}$ values = -0.4‰ to 6.4‰). Moreover, there is an increasing trend in $\delta^{18}O$ values from stratiform-type ore to vein-type ore (Table 2).

4 DISCUSSION

4.1 Sources of S and Pb

Sulfide mineral assemblage is simple at Binh Do, and comprises mainly galena, sphalerite and pyrite. No barite, alunite, gypsum or other sulfate minerals are present, suggesting that the ore-forming fluids occurred mainly in the form of HS^- and S^{2-} (Ohmoto, 1972). In addition, the symbiotic relationship and hypidiomorphic-xenomorphic textures of these sulfide minerals indicate that they were precipitated almost simultaneously. Therefore, the sulfur isotopes of sulfides can approximate those of the ore fluids. In addition, the S isotopic ranges of all sulfides are relatively narrow ($\delta^{34}S$= +1.3‰ to +6.2‰) and peaked at ~2 (Fig. 5a), implying that the ore-forming fluid had reached equilibrium in S isotope. This is further evidenced by the enrichment of ^{34}S order ($\delta^{34}S_{pyrite}$> $\delta^{34}S_{sphalerite}$>$\delta^{34}S_{galena}$) which is in accordance with the order of equilibrium of thermodynamic fractionation of sulfur isotopes in mineral phase (Ohmoto, 1986; Rye and Ohmoto, 1974).

Since the sulfur isotope had reached equilibrium, fractionation equations can be used to calculate the temperature of the symbiotic mineral formations (Rye and Ohmoto, 1974). In this study, the temperatures of mineral pairs (pyrite-sphalerite and sphalerite-galena) are calculated at 172.2 to 277.8 °C and

Table 1 S and Pb isotope composition of ore minerals from Binh Đo deposit

Sample No.	Lithology	Mineral	$\delta^{34}S_{CDT}$ (‰)	$^{206}Pb/^{204}Pb$	$^{207}Pb/^{204}Pb$	$^{208}Pb/^{204}Pb$	μ	ω	Th/U	t (Ma)
FL002	Bedded ore-body	Galena	2.3	18.633	15.779	39.363	9.79	40.78	4.03	226
		Sphalerite	3.9	18.553	15.742	39.139	9.73	39.96	3.97	238
		Pyrite	6.2							
FL014	Bedded ore-body	Galena	3.1	18.673	15.798	39.428	9.83	41.00	4.12	221
		Sphalerite	2.7	18.586	15.752	39.165	9.74	39.97	3.97	227
		Pyrite	5.8							
FL015	Vein ore body	Galena	2.3	18.593	15.762	39.241	9.76	40.34	4.00	234
		Sphalerite	3.1	18.658	15.788	39.414	9.81	40.93	4.04	220
		Pyrite	5.4							
FL022	Vein ore body	Galena	1.3	18.501	15.707	38.911	9.66	38.97	3.90	233
		Sphalerite	3.6	18.622	15.767	39.318	9.77	40.54	4.02	220
		Pyrite	4.9							

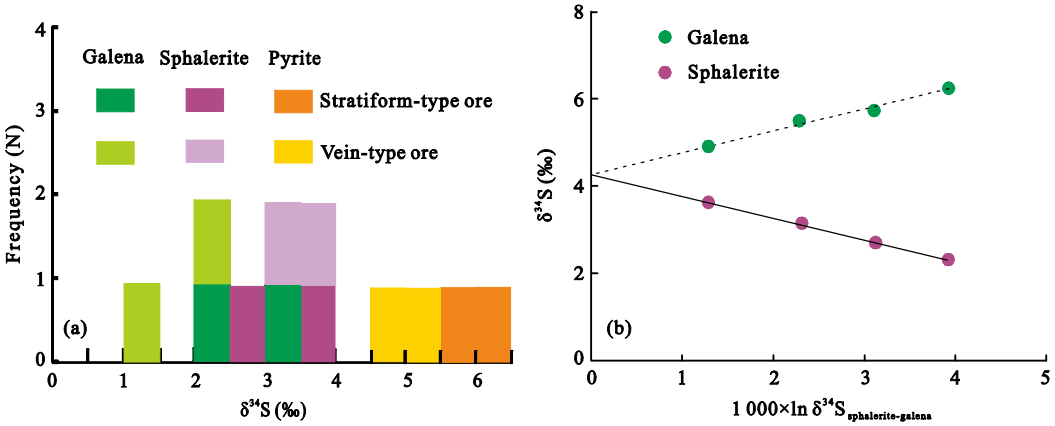

Figure 5. (a) Histogram of S isotopes and (b) 1 000×ln $\delta^{34}S_{sphalerite\text{-}galena}$ vs. $\delta^{34}S$ diagram (after Pinckney and Rafter, 1972) for sulfide minerals from the Binh Do Pb-Zn deposit.

Table 2 Hydrogen and oxygen isotopic compositions of the Binh Đo Pb-Zn deposit

Sample No.	Lithology	Mineral	$\delta D_{V\text{-}SMOW}$ (‰)	$\delta O_{V\text{-}SMOW}$ (‰)	δO_{H2O} (‰)	Temperature (°C)
FL002	Bedded ore-body	Quartz	-75.3	10.4	0.4	230
FL004	Bedded ore-body	Quartz	-82.4	10.5	0.5	230
FL011	Bedded ore-body	Quartz	-73.6	9.6	-0.4	230
FL015	Vein ore body	Quartz	-78.2	10.2	0.2	230
FL017	Vein ore body	Quartz	-70.5	15.3	5.3	230
FL022	Vein ore body	Quartz	-77.8	16.4	6.4	230

157.1 to 272.2 °C, respectively (mean ~230 °C). These results show that these minerals were formed under similar temperature and chemical conditions. Therefore, the method from Pinckney and Rafter (1972) can be used to further determine the average isotopic composition of total sulfur ($\delta^{34}S_{\sum S}$) in the ore-forming fluids. As shown in Fig. 5b, the average ore fluid $\delta^{34}S_{\sum S}$ value (+4.3‰) is close to the magmatic sulfur ($\delta^{34}S$= 0±3‰), and thus the sulfur may have been magma-derived.

Compared with the $\delta^{34}S$ of different deposit types, the Binh Do data are markedly different from those of typical MVT-type Pb-Zn deposits (e.g., the Xiangxi deposit, $\delta^{34}S$= +11.0‰ to +31.4‰; Zhang et al., 2005) but similar to the granite intrusion-related Cho Dìen Pb-Zn deposit in the northern Vietnam Pb-Zn belt ($\delta^{34}S$= +4.1‰ to +6.8‰; Wang et al., 2015) and in the other Pb-Zn belts (Huang et al., 2019; Liu et al., 2018; Xing et al., 2016; Corsini et al., 1980). Therefore, the sulfur of the Binh Do Pb-Zn ores was likely derived from buried intrusive bodies.

Lead isotope compositions of the Binh Do ore sulfides are featured by their narrow range (<1%), suggestive of a single or highly similar Pb source. The Th/U ratios of the sulfides range from 3.9 and 4.0, similar to the average Th/U ratios of mainland China (4.20±0.13; Zhu et al., 1998), indicating an affinity of Pb source between the northern Vietnam Pb-Zn belt and the South China Block. The Th/U ratios and ω and μ values are close to those of typical magmatic-hydrothermal Pb-Zn deposits in South

China (e.g., the Fulaichang Pb-Zn deposit in Guizhou; Tang et al., 2012). This suggests that the Pb isotopes of the Binh Do Pb-Zn deposit is characterized by a single-stage common Pb composition, and its model age may represent the Pb-Zn ore-forming age. In the Pb isotope discrimination diagram (Figs. 6a, 6b), the Binh Do data all plot near or above the upper crustal curve, indicating an upper crustal source. This is further evidenced by the $\Delta\beta$-$\Delta\gamma$ diagram (Fig. 6c), on which all the sample data fall inside the field of supracrustal lead. The Pb isotope model ages of the Binh Do sulfides (240 to 220 Ma) are younger than the Upper Paleozoic wall-rocks, but similar to those of the Early Triassic granitoids in northern Vietnam. In northern Vietnam, the extensive Indosinian (Triassic: ca. 250 to 220 Ma) peraluminous S-type granitic magmatism is widely regarded to have been derived from upper crust remelting (Chen et al., 2014, 2013; Roger et al., 2012). These S-type granites may have contributed (at least part of) the metals to Binh Do, although Triassic intrusions are yet to be found in the mining area at the present exploration depths.

4.2 Fluid Characteristics and Ore Genesis

Hydrogen and oxygen isotopes can effectively identify the ore-forming fluid source. The δD values (Table 2) of the Binh Do ore-forming fluids fall inside the magmatic water field (-80‰ to -40‰), indicating that the ore-forming fluids may have been magma-derived. In the δD vs. $\delta^{18}O_{H2O}$ diagram (Fig. 6d), the Binh Do data plot between the magmatic water and the meteoric water line, but closer to the former. Integrated with the S-Pb isotope results, it is inferred that the Binh Do ore-forming fluids were likely magmatic-derived, probably mixed with some meteoric water.

Ore-forming temperature is also a good indicator to differentiate different types of Pb-Zn deposits. Basinal brines-derived MVT-type Pb-Zn deposits are commonly characterized by low ore-forming temperatures (90 to 150 °C) (Leach et al., 2010, 2005; Basuki, 2008, 2002), which are considerably lower than the temperature (mean 230 °C) calculated from the S isotope data of sulfide mineral pairs at Binh Do. The H-O isotope characteristics of the Binh Do Pb-Zn ores (esp. vein-type) are quite similar to those of the magmatic-hydrothermal type Pb-Zn deposits in Guangxi (South China) (Zhou et al., 2018; Chai et al., 2015), further supporting that the ore-forming fluids were mainly magmatic-hydrothermal with minor meteoric water input.

The Binh Do Pb-Zn deposit is hosted mainly in carbonate rocks, composed of stratiform-type and vein-type orebodies that are controlled by faults and fractured zones, and no magmatic rocks are outcropped. These features are highly similar to

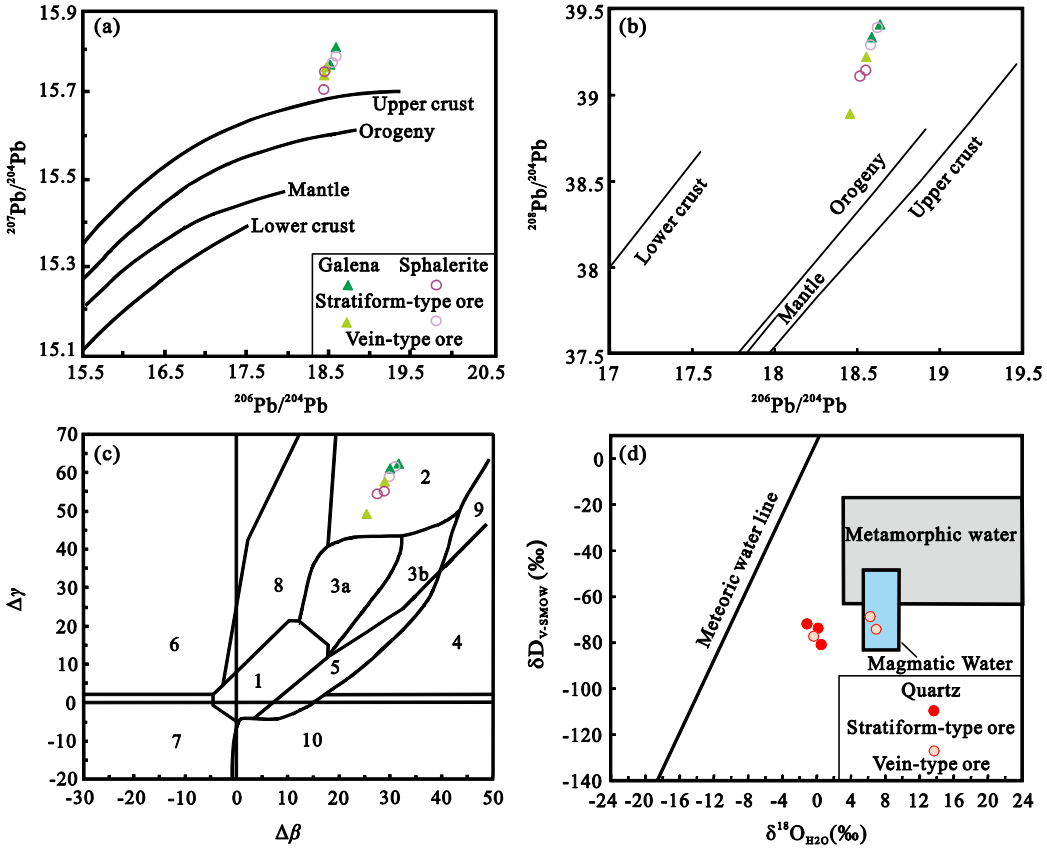

Figure 6. (a) $^{207}Pb/^{204}Pb$ vs. $^{206}Pb/^{204}Pb$ diagram, (b) $^{208}Pb/^{204}Pb$ vs. $^{206}Pb/^{204}Pb$ diagram, (c) $\Delta\beta$ vs. $\Delta\gamma$ diagram (after Zhu et al., 1998), and (d) $\delta D_{V\text{-}SMOW}$ vs. $\delta^{18}O_{H2O}$ diagram of the Binh Do Pb-Zn deposit. In (c): 1. Mantle lead; 2. supracrustal lead; 3a, 3b. mixed supracrustal and mantle lead (magmatism); 4. chemical deposit lead; 5. submarine hydrothermal lead; 6. metamorphic lead (medium-grade metamorphism); 7. metamorphic (lower crust) lead (high-grade metamorphism); 8. orogenic lead; 9. ancient shale (upper crust) lead; 10. retrograde metamorphism lead. $\Delta\beta$ and $\Delta\gamma$ are relative deviations between contemporaneous mantle values and $^{207}Pb/^{204}Pb$ and $^{208}Pb/^{204}Pb$ ratios, respectively. The lead isotope curves for the mantle, orogeny, upper crust, and lower crust are from Zartman and Doe (1981). The base diagram of H-O isotopes is from Taylor (1974).

the other Pb-Zn deposits in northern Vietnam, such as the Bình Chai, Lũng Hoài and Po Pen deposits (Anh et al., 2012; Ishihara et al., 2010; Tran et al., 2008). Opinions vary on the metallogenic style of the northern Vietnam Pb-Zn belt: previous local researchers argued that the carbonate-hosted stratiform Pb-Zn orebodies are similar to typical MVT Pb-Zn deposits, whereas Anh et al. (2012) suggested that although no intrusions are exposed in most of the Pb-Zn deposits, the strong coeval magmatism may have been genetically linked with the regional Pb-Zn mineralization. Through systematic and laboratory studies, we found that there are obvious differences in many aspects between the Binh Do Pb-Zn deposit and the typical MVT or SEDEX deposits (Li K et al., 2018; Sun et al., 2017a; Li and Xi, 2015). We propose that concealed intrusions may have provided the fluids, metals and heat for the Binh Do Pb-Zn mineralization. Our field observations reveal a clear mineral zoning pattern at Binh Do, where the lower-temperature assemblage of sphalerite+galena+pyrite passes downward to the higher-temperature assemblage of pyrrhotite+scheelite. This zoning pattern of increasing temperature with depth is atypical in sedimentary-type (MVT or SEDEX) Pb-Zn deposits but common in magmatic-hydrothermal W-Sn-Pb-Zn polymetallic deposits (e.g., Jiang et al., 2018; Li et al., 2018c, d, 2017, 2014a, b; Wu et al., 2018; Sun et al., 2017b.), thus implying a heat-source (probably intrusion) at depth and suggesting a magmatic-hydrothermal origin for the Binh Do Pb-Zn mineralization.

4.3 Metallogenic Model

It is noticeable that there are some regular variations of S-Pb-H-O isotopes from vein-type ores to stratiform-type ores: $\delta^{34}S$ values decrease whereas $^{18}O_{V\text{-}SMOW}$ values increase, and $^{206}Pb/^{204}Pb$, $^{207}Pb/^{204}Pb$ and $^{208}Pb/^{204}Pb$ ratios increase in galena whereas decrease in sphalerite (Tables 1 and 2). This may indicate a time sequence of the mineralization in the Binh Do deposit, resulting in the vein-type and stratiform-type ores successively (i.e., vein-type ores might be formed slightly earlier than the stratiform-type ores). In the granite intrusion-related hydrothermal systems, $\delta^{34}S$ values normally increase whereas $^{18}O_{V\text{-}SMOW}$ values decrease along with the mineralization processes, whereas Pb/Pb ratios may differ among intergrown minerals (Li et al., 2018b). The higher $\delta^{34}S$ values for the sulfides from the stratiform-type ores could be a product of quantitative BSR (bacterial sulfate reduction), but it is more likely that thermochemical sulfate reduction of seawater sulfate or of evaporite (related with the carbonate rocks) was the source of heavy hydrothermal sulfur (Ma et al., 2004). This may indicate an increased stratigraphic control but decreased magmatic impact with the advance of ore-forming process. The decreased $^{18}O_{V\text{-}SMOW}$ values from vein-type ores to stratiform-type ores also support this inference (Fig. 6d). Overall, the slightly different but overall consistent values of these isotopes in the Binh Do deposit also suggest that the vein-type ores to stratiform-type ores have the similar source of ore-forming materials but precipitated successively in different structures.

Combined the S-Pb-H-O isotopic data with field observations and previous literature, we propose a metallogenic model for the northern Vietnam Pb-Zn belt (Fig. 7): In the Early Triassic, northern Vietnam may have collided with the Indochina Block and underwent the Indosinian orogenic events. Under the strong extrusion environment, partial melting of the thickened crust resulted in large-scale emplacement of post-orogenic S-type granites, providing massive heat and ore-forming materials. Meanwhile, the multi-level and multi-scale faults are reactivated, providing channels for the migration of the magmatic-hydrothermal fluids. The good permeability of the carbonate rocks has given impetus to the migration and precipitation of the hydrothermal fluids. The final deposition of the Pb-Zn materials was caused by the mixing of deep-seated magma-derived fluid with meteoric water in the shallower crust, forming the vein-type and stratiform-type Pb-Zn orebodies successively.

5 CONCLUSIONS

(1) The Binh Do Pb-Zn stratiform-/vein-type orebodies are hosted in Upper Paleozoic carbonate rocks. The $\delta^{34}S$ values range from +1.3% to +6.2% ($\delta^{34}S_{pyrite}>\delta^{34}S_{sphalerite}>\delta^{34}S_{galena}$), indicating a magmatic sulfur with an equilibrized ore-forming

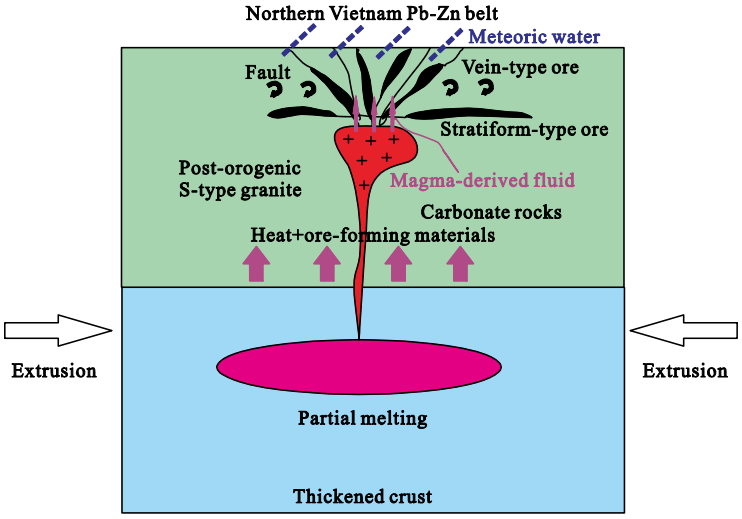

Figure 7. A genetic model to explain the ore-forming process of the Binh Do Pb-Zn deposit, northern Vietnam Pb-Zn belt.

temperature of ~230 ºC.

(2) Lead isotope compositions of the Binh Do ore sulfides are similar, suggesting a homogeneous upper crustal lead source. The one-stage Pb model age is ca. 238 to 220 Ma, broadly coeval with the regional Triassic (Indosinian) S-type granitic magmatism. Isotope evidence and vertical ore mineral zoning pattern suggest the ore-forming fluids, metals and heat may have originated from concealed S-type granites in the area.

(3) The $\delta D_{V\text{-}SMOW}$ and $\delta^{18}O_{H_2O}$ values of the ore-related quartz range -82.4‰ to -70.5‰ and -0.4‰ to +6.4‰, respectively, indicating that the ore-forming fluids were mainly magmatic-hydrothermal derived with minor meteoric water input.

(4) We suggest that the Binh Do Pb-Zn deposit is best attributed to be magmatic-hydrothermal type, rather than MVT type as previously proposed.

ACKNOWLEDGMENTS

We thank Mr. Tianguo Wang for his help in sample collection. This work was partially financed by the National Natural Science Foundation of China (No. 41502067). The editor and anonymous reviewers are thanked for the insightful comments and suggestions. The final publication is available at Springer via https://doi.org/10.1007/s12583-019-0872-2.

REFERENCES CITED

Anh, T. T., Gas'Kov, I. V., Hoa, T. T., et al., 2012. Complex Deposits in the Lo Gam Structure, Northeastern Vietnam: Mineralogy, Geochemistry, and Formation Conditions. *Russian Geology and Geophysics*, 53(7): 623–635. https://doi.org/10.1016/j.rgg.2012.05.001

Basuki, N. I., 2002. A Review of Fluid Inclusion Temperatures and Salinities in Mississippi Valley-Type Zn-Pb Deposits: Identifying Thresholds for Metal Transport. *Exploration and Mining Geology*, 11(1/2/3/4): 1–17. https://doi.org/10.2113/11.1-4.1

Basuki, N. I., Taylor, B. E., Spooner, E. T. C., 2008. Sulfur Isotope Evidence for Thermochemical Reduction of Dissolved Sulfate in Mississippi Valley-Type Zinc-Lead Mineralization, Bongara Area, Northern Peru. *Economic Geology*, 103(4): 783–799. https://doi.org/10.2113/gsecongeo.103.4.783

Cai, J. X., Zhang, K. J., 2009. A New Model for the Indochina and South China Collision during the Late Permian to the Middle Triassic. *Tectonophysics*, 467(1/2/3/4): 35–43. https://doi.org/10.1016/j.tecto.2008.12.003

Can, P. N., Ishiyama, D., Anh, T. T., et al., 2011. Mineralogical and Geochemical Characteristics of Rare Metals-Bearing Na Bop, Lung Hoai, Na Son and Sin Quyen Base Metal Deposits, Northern Vietnam. *NMCC Annual Report*, 18: 49−55

Carter, A., Roques, D., Bristow, C., et al., 2001. Understanding Mesozoic Accretion in Southeast Asia: Significance of Triassic Thermotectonism (Indosinian Orogeny) in Vietnam. *Geology*, 29(3): 211−214. https://doi.org/10.1130/0091-7613(2001)029<0211:umaisa>2.0.co;2

Chai, M. C., Wei, F. U., Feng, Z. H., et al., 2015. Characteristics of Ore-Forming Fluids of Nongtun Pb-Zn Deposit in Xidaming Mountain of Guangxi and Their Implications for Ore Genesis. *Mineral Deposits*, 34(5): 948−964 (in Chinese with English Abstract)

Chen, Z. C., Lin, W., Faure, M., et al., 2013. Geochronological Constraint of Early Mesozoic Tectonic Event at Northeast Vietnam. *Acta Petrologica Sinica*, 29(5): 1825−1840 (in Chinese with English Abstract)

Chen, Z. C., Lin, W., Faure, M., et al., 2014. Geochronology and Isotope Analysis of the Late Paleozoic to Mesozoic Granitoids from Northeastern Vietnam and Implications for the Evolution of the South China Block. *Journal of Asian Earth Sciences*, 86: 131–150. https://doi.org/10.1016/j.jseaes.2013.07.039

Cheng, Y. B., Mao, J. W., Liu, P., 2016. Geodynamic Setting of Late Cretaceous Sn-W Mineralization in Southeastern Yunnan and Northeastern Vietnam. *Solid Earth Sciences*, 1(3): 79–88. https://doi.org/10.1016/j.sesci.2016.12.001

Corsini, F., Cortecci, G., Leone, G., et al., 1980. Sulfur Isotope Study of the Skarn-(Cu-Pb-Zn) Sulfide Deposit of Valle Del Temperino, Campiglia Marittima, Tuscany, Italy. *Economic Geology*, 75(1): 83–96. https://doi.org/10.2113/gsecongeo.75.1.83

Findlay, R. H., 1997. The Song Ma Anticlinorium, Northern Vietnam: The Structure of an Allochthonous Terrane Containing an Early Palaeozoic Island Arc Sequence. *Journal of Asian Earth Sciences*, 15(6): 453–464. https://doi.org/10.1016/s0743-9547(97)00031-7

Gilley, L. D., Harrison, T. M., Leloup, P. H., et al., 2003. Direct Dating of Left-Lateral Deformation along the Red River Shear Zone, China and Vietnam. *Journal of Geophysical Research*: *Solid Earth*, 108(B2): 2127. https://doi.org/10.1029/2001jb001726

Gonez, P., Nguyên Huu, H., Ta Hoa, P., et al., 2012. The Oldest Flora of the South China Block, and the Stratigraphic Bearings of the Plant Remains from the Ngoc Vung Series, Northern Vietnam. *Journal of Asian Earth Sciences*, 43(1): 51–63. https://doi.org/10.1016/j.jseaes.2011.08.007

Halpin, J. A., Tran, H. T., Lai, C.-K., et al., 2016. U-Pb Zircon Geochronology and Geochemistry from NE Vietnam: A 'Tectonically Disputed' Territory between the Indochina and South China Blocks. *Gondwana Research*, 34: 254–273. https://doi.org/10.1016/j.gr.2015.04.005

Hanski, E., Walker, R. J., Huhma, H., et al., 2004. Origin of the Permian–Triassic Komatiites, Northwestern Vietnam. *Contributions to Mineralogy and Petrology*, 147(4): 453–469. https://doi.org/10.1007/s00410-004-0567-1

Huang, C. W., Du, G. F., Jiang, H. J., et al., 2019. Ore-Forming Fluids Characteristics and Metallogenesis of the Anjing Hitam Pb-Zn Deposit in Northern Sumatra, Indonesia. *Journal of Earth Science*, 30(1): 131–141. https://doi.org/10.1007/s12583-019-0859-z

Ishihara, S., Anh Tran, T., Watanabe, Y., et al., 2010. Chemical Characteristics of Lead-Zinc Ores from North Vietnam, with a Special Attention to the in Contents. *Bulletin of the Geological Survey of Japan*, 61(9/10): 307–323. https://doi.org/10.9795/bullgsj.61.307

Jiang, W. C., Li, H., Wu, J. H., et al., 2018. A Newly Found Biotite Syenogranite in the Huangshaping Polymetallic Deposit, South China: Insights into Cu Mineralization. *Journal of Earth Science*, 29(3): 537–555. https://doi.org/10.1007/s12583-017-0974-7

Lai, C.-K., Meffre, S., Crawford, A. J., et al., 2014a. The Central Ailaoshan Ophiolite and Modern Analogs. *Gondwana Research*, 26(1): 75–88. https://doi.org/10.1016/j.gr.2013.03.004

Lai, C.-K., Meffre, S., Crawford, A. J., et al., 2014b. The Western Ailaoshan Volcanic Belts and Their SE Asia Connection: A New Tectonic Model for the Eastern Indochina Block. *Gondwana Research*, 26(1): 52–74. https://doi.org/10.1016/j.gr.2013.03.003

Leach, D. L., Bradley, D. C., Huston, D., et al., 2010. Sediment-Hosted Lead-Zinc Deposits in Earth History. *Economic Geology*, 105(3): 593–625. https://doi.org/10.2113/gsecongeo.105.3.593

Leach, D. L., Sangster, D. F., Kelley, K. D., et al., 2005. Sediment-Hosted Lead-Zinc Deposits: A Global Perspective. *Economic Geology*, 100:

561−607. https://doi.org/10.5382/av100.18

Lepvrier, C., Faure, M., Van, V. N., et al., 2011. North-Directed Triassic Nappes in Northeastern Vietnam (East Bac Bo). *Journal of Asian Earth Sciences*, 41(1): 56–68. https://doi.org/10.1016/j.jseaes.2011.01.002

Li, H., Myint, A. Z., Yonezu, K., et al., 2018a. Geochemistry and U-Pb Geochronology of the Wagone and Hermyingyi A-Type Granites, Southern Myanmar: Implications for Tectonic Setting, Magma Evolution and Sn-W Mineralization. *Ore Geology Reviews*, 95: 575–592. https://doi.org/10.1016/j.oregeorev.2018.03.015

Li, H., Palinkaš, L. A., Watanabe, K., et al., 2018d. Petrogenesis of Jurassic A-Type Granites Associated with Cu-Mo and W-Sn Deposits in the Central Nanling Region, South China: Relation to Mantle Upwelling and Intra-Continental Extension. *Ore Geology Reviews*, 92: 449–462. https://doi.org/10.1016/j.oregeorev.2017.11.029

Li, H., Watanabe, K., Yonezu, K., 2014a. Zircon Morphology, Geochronology and Trace Element Geochemistry of the Granites from the Huangshaping Polymetallic Deposit, South China: Implications for the Magmatic Evolution and Mineralization Processes. *Ore Geology Reviews*, 60: 14–35. https://doi.org/10.1016/j.oregeorev.2013.12.009

Li, H., Watanabe, K., Yonezu, K., 2014b. Geochemistry of A-Type Granites in the Huangshaping Polymetallic Deposit (South Hunan, China): Implications for Granite Evolution and Associated Mineralization. *Journal of Asian Earth Sciences*, 88: 149–167. https://doi.org/10.1016/j.jseaes.2014.03.004

Li, H., Wu, J. H., Evans, N. J., et al., 2018c. Zircon Geochronology and Geochemistry of the Xianghualing A-Type Granitic Rocks: Insights into Multi-Stage Sn-Polymetallic Mineralization in South China. *Lithos*, 312/313: 1–20. https://doi.org/10.1016/j.lithos.2018.05.001

Li, H., Wu, Q. H., Evans, N. J., et al., 2018b. Geochemistry and Geochronology of the Banxi Sb Deposit: Implications for Fluid Origin and the Evolution of Sb Mineralization in Central-Western Hunan, South China. *Gondwana Research*, 55: 112–134. https://doi.org/10.1016/j.gr.2017.11.010

Li, H., Xi, X. S., 2015. Sedimentary Fans: A New Genetic Model for Sedimentary Exhalative Ore Deposits. *Ore Geology Reviews*, 65: 375–389. https://doi.org/10.1016/j.oregeorev.2014.10.001

Li, H., Xi, X. S., Sun, H. S., et al., 2016. Geochemistry of the Batang Group in the Zhaokalong Area, Yushu, Qinghai: Implications for the Late Triassic Tectonism in the Northern Sanjiang Region, China. *Acta Geologica Sinica*: *English Edition*, 90(2): 704–721. https://doi.org/10.1111/1755-6724.12699

Li, H., Xi, X. S., Wu, C. M., et al., 2013. Genesis of the Zhaokalong Fe-Cu Polymetallic Deposit at Yushu, China: Evidence from Ore Geochemistry and Fluid Inclusions. *Acta Geologica Sinica*: *English Edition*, 87(2): 486–500. https://doi.org/10.1111/1755-6724.12063

Li, H., Yonezu, K., Watanabe, K., et al., 2017. Fluid Origin and Migration of the Huangshaping W-Mo Polymetallic Deposit, South China: Geochemistry and $^{40}Ar/^{39}Ar$ Geochronology of Hydrothermal K-Feldspars. *Ore Geology Reviews*, 86: 117–129. https://doi.org/10.1016/j.oregeorev.2017.02.005

Li, K., Zhao, S., Tang, Z., et al., 2018. Fluid Sources and Ore Genesis of the Pb-Zn Deposits of Huayuan Ore-Concentrated District, Northwest Hunan Province, China. *Earth Science*, 43(7), 2449–2464 (in Chinese with English Abstract)

Liu, W. H., Zhang, X. J., Zhang, J., et al., 2018. Sphalerite Rb-Sr Dating and *In Situ* Sulfur Isotope Analysis of the Daliangzi Lead-Zinc Deposit in Sichuan Province, SW China. *Journal of Earth Science*, 29(3): 573–586. https://doi.org/10.1007/s12583-018-0785-5

Liu, Y. P., Li, Z. X., Li, H. M., et al., 2007. U-Pb Geochronology of Cassiterite and Zircon from the Dulong Sn-Zn Deposit: Evidence for Cretaceous Large-Scale Granitic Magmatism and Mineralization Events in Southeastern Yunnan Province, China. *Acta Petrologica Sinica*, 23(5): 967−976 (in Chinese with English Abstract)

Lu, Y. X., Liu, H. G., Huang, J. N., et al., 2009. Preliminary Division of the Metallogenetic Belts in the Central South Peninsula of Southeast Asia and Their Regional Ore-Forming Characteristics. *Geological Bulletin of China*, 28 (2/3): 314−325 (in Chinese with English Abstract)

Ma, G. L., Beaudoin, G., Qi, S. J., et al., 2004. Geology and Geochemistry of the Changba SEDEX Pb-Zn Deposit, Qinling Orogenic Belt, China. *Mineralium Deposita*, 39(3): 380–395. https://doi.org/10.1007/s00126-004-0416-1

Metcalfe, I., 2002. Permian Tectonic Framework and Palaeogeography of SE Asia. *Journal of Asian Earth Sciences*, 20(6): 551–566. https://doi.org/10.1016/s1367-9120(02)00022-6

Ni, P., Wang, G. G., Cai, Y. T., et al., 2017. Genesis of the Late Jurassic Shizitou Mo Deposit, South China: Evidences from Fluid Inclusion, H O Isotope and Re Os Geochronology. *Ore Geology Reviews*, 81: 871–883. https://doi.org/10.1016/j.oregeorev.2016.08.013

Ohmoto, H., 1972. Systematics of Sulfur and Carbon Isotopes in Hydrothermal Ore Deposits. *Economic Geology*, 67(5): 551–578. https://doi.org/10.2113/gsecongeo.67.5.551

Ohmoto, H., 1986. Stable Isotope Geochemistry of Ore Deposits. *Reviews in Mineralogy and Geochemistry*, 16(1): 491−559

Pham-Ngoc, C., Ishiyama, D., Tran, T. A., et al., 2016. Characteristic Features of REE and Pb-Zn-Ag Mineralizations in the Na Son Deposit, Northeastern Vietnam. *Resource Geology*, 66(4): 404–418. https://doi.org/10.1111/rge.12110

Pinckney, D. M., Rafter, T. A., 1972. Fractionation of Sulfur Isotopes during Ore Deposition in the Upper Mississippi Valley Zinc-Lead District. *Economic Geology*, 67(3): 315–328. https://doi.org/10.2113/gsecongeo.67.3.315

Polyakov., G. V., Tran, T. H., Akimtsev, V. A., et al., 1999. Ore and Geochemical Specialization of Permo-Triassic Ultramafic-Mafic Complexes in North Vietnam. *Geologiya I Geofizika*, 40(10): 1474–1487

Roger, F., Leloup, P. H., Jolivet, M., et al., 2000. Long and Complex Thermal History of the Song Chay Metamorphic Dome (Northern Vietnam) by Multi-System Geochronology. *Tectonophysics*, 321(4): 449–466. https://doi.org/10.1016/s0040-1951(00)00085-8

Roger, F., Maluski, H., Lepvrier, C., et al., 2012. LA-ICPMS Zircons U/Pb Dating of Permo-Triassic and Cretaceous Magmatisms in Northern Vietnam-Geodynamical Implications. *Journal of Asian Earth Sciences*, 48: 72–82. https://doi.org/10.1016/j.jseaes.2011.12.012

Rye, R. O., Ohmoto, H., 1974. Sulfur and Carbon Isotopes and Ore Genesis: A Review. *Economic Geology*, 69(6): 826–842. https://doi.org/10.2113/gsecongeo.69.6.826

Sun, H. S., Li, H., Danišík, M., et al., 2017b. U-Pb and Re-Os Geochronology and Geochemistry of the Donggebi Mo Deposit, Eastern Tianshan, NW China: Insights into Mineralization and Tectonic Setting. *Ore Geology Reviews*, 86: 584–599. https://doi.org/10.1016/j.oregeorev.2017.03.020

Sun, H. S., Li, H., Evans, N. J., et al., 2017a. Volcanism, Mineralization and Metamorphism at the Xitieshan Pb-Zn Deposit, NW China: Insights from Zircon Geochronology and Geochemistry. *Ore Geology Reviews*, 88: 289–303. https://doi.org/10.1016/j.oregeorev.2017.05.010

Tan, J., Liu, C., Yang, H., et al., 2018. Geochronology and Ore-Forming Material Source Constraints for Rouxianshan Pb-Zn Deposit in Hua-

yuan Ore Concentration Area, Western Hunan. *Earth Science*, 43(7): 2438–2448 (in Chinese with English Abstract)

Tang, S., Ma, X., Li, X., et al., 2012. Pb Isotope Composition of the Fulaichang Lead-Zinc Ore Deposit in Northwest Guizhou and Its Geological Implications. *Geotectonica et Metallogenia*, 36(4): 549–558 (in Chinese with English Abstract)

Taylor, H. P., 1974. The Application of Oxygen and Hydrogen Isotope Studies to Problems of Hydrothermal Alteration and Ore Deposition. *Economic Geology*, 69(6): 843–883. https://doi.org/10.2113/gsecongeo.69.6.843

Todt, W., Cliff, R. A., Hanser, A., et al., 1996. Evaluation of a ^{202}Pb-^{205}Pb Double Spike for High-Precision Lead Isotope Analysis. *Geophysical Monograph Series*, 95: 429–437. https://doi.org/10.1029/gm095p0429

Tran, T. H., Izokh, A. E., Polyakov, G. V., et al., 2008. Permo-Triassic Magmatism and Metallogeny of Northern Vietnam in Relation to the Emeishan Plume. *Russian Geology and Geophysics*, 49(7): 480–491. https://doi.org/10.1016/j.rgg.2008.06.005

Wang, D. S., Liu, J. L., Mydung, T., et al., 2011. Geochronology, Geochemistry and Tectonic Significance of Granites in the Tinh Túc W-Sn Ore Deposits, Northeast Vietnam. *Acta Petrologica Sinica*, 27(9): 2795−2808 (in Chinese with English Abstract)

Wang, D. S., Liu, J. L., Tran, M. D., et al., 2015. Sulfur and Lead Isotope Compositions of Sulfides in the Cho Dìen Pb-Zn Deposit, Northeast Vietnam, and Their Geological Implications. *Geological Bulletin of China*, 34(4): 757−768 (in Chinese with English Abstract)

Won-In, K., Charusiri, P., 2003. Enhancement of Thematic Mapper Satellite Images for Geological Mapping of the Cho Dien Area, Northern Vietnam. *International Journal of Applied Earth Observation and Geoinformation*, 4(3): 183–193. https://doi.org/10.1016/s0303-2434(02)00034-x

Wu, J. H., Li, H., Algeo, T. J., et al., 2018. Genesis of the Xianghualing Sn-Pb-Zn Deposit, South China: A Multi-Method Zircon Study. *Ore Geology Reviews*, 102: 220–239. https://doi.org/10.1016/j.oregeorev.2018.09.005

Xia, X. P., Nie, X. S., Lai, C.-K., et al., 2016. Where was the Ailaoshan Ocean and when did It Open: A Perspective Based on Detrital Zircon U-Pb Age and Hf Isotope Evidence. *Gondwana Research*, 36: 488–502. https://doi.org/10.1016/j.gr.2015.08.006

Xing, B., Xiang, J. F., Ye, H. S., et al., 2016. Rb-Sr Isochron Age of Sulfides and Sulfur Isotopic Composition from Lamellar Ores of the Luotuoshan Sulfur Polymetallic Deposit in Western Henan Province and Its Constraints on the Ore Genesis. *Geological Bulletin of China*, 35(6): 998−1014 (in Chinese with English Abstract)

Xu, B., Jiang, S. Y., Luo, L., et al., 2017. Origin of the Granites and Related Sn and Pb-Zn Polymetallic Ore Deposits in the Pengshan District, Jiangxi Province, South China: Constraints from Geochronology, Geochemistry, Mineral Chemistry, and Sr-Nd-Hf-Pb-S Isotopes. *Mineralium Deposita*, 52(3): 337–360. https://doi.org/10.1007/s00126-016-0659-7

Yan, D. P., Zhou, M. F., Song, H. L., et al., 2003. Origin and Tectonic Significance of a Mesozoic Multi-Layer Over-Thrust System within the Yangtze Block (South China). *Tectonophysics*, 361(3/4): 239–254. https://doi.org/10.1016/s0040-1951(02)00646-7

Yan, D. P., Zhou, M. F., Wang, C. Y., et al., 2006. Structural and Geochronological Constraints on the Tectonic Evolution of the Dulong-Song Chay Tectonic Dome in Yunnan Province, SW China. *Journal of Asian Earth Sciences*, 28(4/5/6): 332–353. https://doi.org/10.1016/j.jseaes.2005.10.011

Zartman, R. E., Doe, B. R., 1981. Plumbotectonics—The Model. *Tectonophysics*, 75(1/2): 135–162. https://doi.org/10.1016/0040-1951(81)90213-4

Zhang, C. Q., Mao J. W., Wu, S. P., et al., 2005. Distribution, Characteristics and Genesis of Mississippi Valley-Type Lead Zinc Deposits in Sichuan-Yunnan-Guiz Hou Area. *Mineral Deposits*, 24(3): 336−348 (in Chinese with English Abstract)

Zhou, J. X., Xiang, Z. Z., Zhou, M. F., et al., 2018. The Giant Upper Yangtze Pb-Zn Province in SW China: Reviews, New Advances and a New Genetic Model. *Journal of Asian Earth Sciences*, 154: 280–315. https://doi.org/10.1016/j.jseaes.2017.12.032

Zhu, B. Q., Li, X. H., Dai, T. M., 1998. Isotope System Theory and Application to the Earth Sciences: On Crust-Mantle Evolution of Continent of China. Science Press, Beijing. 330 (in Chinese)